Journal of Organometallic Chemistry 695 (2010) 1353–1362

Contents lists available at ScienceDirect

Journal of Organometallic Chemistry

journal homepage: www.elsevier.com/locate/jorganchem

New di- and triorganotin(IV) complexes of tripodal Schiff base ligand containing three imidazole arms: Synthesis, structural characterization, anti-inflammatory activity and thermal studies

Mala Nath [a,*], Pramendra Kumar Saini [a], Ashok Kumar [b]

[a] Department of Chemistry, Indian Institute of Technology Roorkee, Roorkee 247667, Uttarakhand, India
[b] Department of Pharmacology, LLRM Medical College, Meerut 250004, India

ARTICLE INFO

Article history:
Received 23 December 2009
Received in revised form 5 February 2010
Accepted 10 February 2010
Available online 16 February 2010

Keywords:
Tripodal Schiff base
Organotin(IV) compounds
Anti-inflammatory activity
Thermal studies

ABSTRACT

Some new tri- and diorganotin(IV) complexes of the general formula, $R_3Sn(H_2L)$ and $R'_2Sn(HL)$ [where R = Me, *n*-Pr, *n*-Bu and Ph; R′ = Me, *n*-Bu, Ph and *n*-Oct; H_3L = Schiff base (abbreviated as tren(4-Me-5-ImH)$_3$) derived from condensation of tris(2-aminoethyl)amine (tren) and 4-methyl-5-imidazolecarboxaldehyde (4-Me-5-ImH)] have been synthesized. The coordination behaviour of Schiff base towards organotin(IV) moieties is discussed on the basis of infrared and far-infrared, ^{119}Sn Mössbauer and multinuclear (^{1}H, ^{13}C and ^{119}Sn) magnetic resonance (NMR) spectroscopic studies. Thermal studies of all of the synthesized organotin(IV) complexes have been carried out using TG, DTG and DTA techniques. The residues thus obtained from pyrolysis of the studied complexes have been characterized by X-ray powder diffraction analysis and IR. The newly synthesized complexes have been tested for their anti-inflammatory activity and toxicity (LD_{50}).

1. Introduction

There has been considerable interest in the synthesis of ligands containing an imidazole moiety because of its biological significance in a variety of metalloproteins, especially heme proteins. Tripodal hexadentate Schiff base ligands formed by the condensation of polyfunctional amine such as tris(2-aminoethyl)amine (tren) and imidazolecarboxaldehyde are capable of chelating a transition metal via imine and deprotonated imidazole N donors. The presence of ionizable protons on the imidazole rings of the several imidazolecarboxaldehyde precursors and substituted imidazolecarboxaldehyde precursors afforded an opportunity to synthesize the complexes of transition metals in various combinations of oxidation and spin states of metal atom and protonation states of the ligands [1–6]. The tripodal Schiff base ligand containing three imidazole groups is the first ligand affording spin-cross over (SCO) behavior for both the Fe^{II} and Fe^{III} oxidation states, and 2D extended network structure based on imidazole–imidazolate hydrogen bonds produces elastic interactions between SCO sites. These ligands can bind to iron with or without ionization of the imidazole ring. It has also been reported that the degree of deprotonation at imidazole moiety and the substituent effect control the oxidation and spin states [1–9].

A number of iron(II, III) complexes of tripodal ligands formed by condensation of tris(2-aminoethyl)amine (tren) with three molar equivalents of 2-imidazolecarboxaldehyde/1-methyl-2-imidazolecarboxaldehyde/2-methyl-4-imidazolecarboxaldehyde/4-methyl-5-imidazolecarboxaldehyde have been reported to show low-spin–high-spin cross over phenomenon [1–10]. Further, the counter anion has been reported to modify the SCO behavior of these 2D complexes through interlayer elastic interactions [8]. Asymmetric tripodal iron complexes of tren and mixtures of aldehydes have also been synthesized and characterized [11]. Recently, Cu(II) and Ni(II) complexes of the type, $[MH_3L](ClO_4)_2$ (where M = Cu(II) and Ni(II), H_3L = Schiff base derived from the condensation of tren and 4-methyl-5-imidazole-carboxaldehyde) have also been reported [12]. The structures of these two complexes are isomorphous with each other and with the iron(II) complex [6]. Further, a neutral complex CuHL and the ionic complex Na[NiL] have also been reported [12]. However, complexes of this type of tripodal Schiff base ligands with main group metals have not been synthesized, and also organotin(IV) complexes of such ligands have not been reported so far.

Recently, the chemistry of organotin(IV) complexes of Schiff bases has stemmed from their antitumour [13–17], antimicrobial [17–20], antinematicidal [21], anti-insecticidal [21] and anti-inflammatory activities [19]. Several organotin(IV) derivatives of dipeptides have been found to exhibit potent anti-inflammatory activity [22–28]. Since fast and effective relief of pain and inflammation in humans with minimum side effects continues to be a

* Corresponding author. Tel.: +91 1332 285797; fax: +91 1332 73560.
E-mail address: malanfcy@iitr.ernet.in (M. Nath).

0022-328X/$ - see front matter © 2010 Published by Elsevier B.V.
doi:10.1016/j.jorganchem.2010.02.009

major challenge for medicinal chemistry researchers. Therefore, from the pharmo-economic point of view, an anti-inflammatory agent with minimum side effects and wider safety margin is highly desirable. In view of this, we report herein synthesis and characterization of tri- and diorganotin(IV) complexes of tripodal Schiff base derived from condensation of tren and 4-methyl-5-imidazolecarboxaldehyde (Fig. 1) along with their anti-inflammatory and toxicity screening studies. Thermal behavior of these complexes has also been included.

2. Experimental

2.1. Materials

All of the syntheses were carried out under an anhydrous nitrogen atmosphere. Dimethyltin(IV) dichloride (Merk-Schuchardt), *n*-dibutyltin(IV) dichloride (Merk-Schuchardt), 4-methyl-5-imidazolecarboxaldehyde (Aldrich), tris(2-aminoethyl)amine (tren) (Aldrich) were used as received. Diphenyltin(IV) dichloride was synthesized according to the reported method [29]. Solvents such as methanol and cyclohexane (Qualigens) were dried and distilled, and stored under nitrogen before use.

2.2. Measurements

The melting points, carbon, hydrogen and nitrogen analysis, conductivity measurements and IR and far-IR spectra of the synthesized complexes were carried out using the same methods and instruments as reported previously [30]. UV spectra of the ligand and its organotin(IV) complexes were recorded on a Shimadzu 1601 UV–vis spectrophotometer in methanol. ^{1}H, ^{13}C{1H} NMR and ^{119}Sn{1H} NMR spectra were recorded at 27 ± 1 °C on a Bruker Avance (500.133 MHz) FT NMR spectrometer equipped with a Quattro probe tuned to 500.133 MHz for ^{1}H, 125.033 MHz for ^{13}C and 186.50 MHz for ^{119}Sn nuclei using CD_3OD as solvent, and TMS (for ^{1}H and ^{13}C NMR) and tetraphenyltin (for ^{119}Sn NMR) as the internal reference at the Indian Institute of Technology Roorkee, Roorkee, India. ^{119}Sn Mössbauer spectrum of $Me_3Sn(L)$ was recorded by a standard Mössbauer spectrometer having 1024 channels (procured from Wissel GmbH, Germany) operating in the constant acceleration mode at UGC-DAE Consortium for Scientific Research, Kolkata, India. The detector used was a proportional counter of LND, USA make. The source used was a 5 milli Curie Sn^{119} in $CaSnO_3$ matrix. The isomer shifts are calculated with respect to the centre of a pure SnO_2 sample procured commercially. The spectra were recorded at 20 K using a closed cycle refrigerator (supplied by Janis Research, USA) coupled to a special anti-vibration stand. Thermal measurements were carried out on a Perkin–Elmer (Pyris Diamond) thermal analyzer in air, in the temperature range 0–1000 °C with heating rate 10 °C/min in a platinum crucible using alumina powder as a reference material at I.I.C., Indian Institute of Technology Roorkee. The X-ray powder diffraction (XRD) of residues obtained by pyrolysis of the studied diorganotin(IV) derivatives of tripodal Schiff base ligand were recorded on a Bruker AXS diffractometer at I.I.C., Indian Institute of Technology Roorkee using nickel monochromated Cu Kα radiation (λ = 1.541 Å).

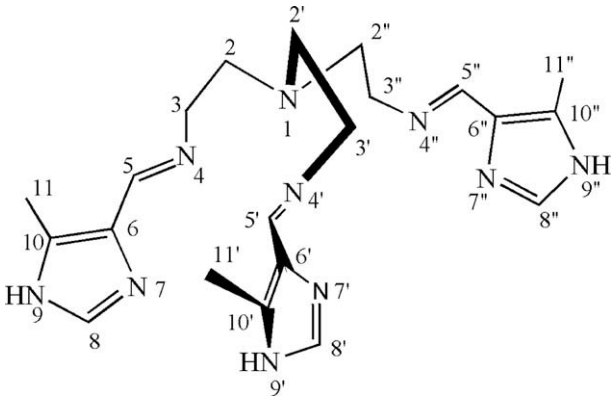

Fig. 1. Chemical structure of Schiff base ligand (tren(4-Me-5-ImH)$_3$) (H_3L).

2.3. Biological studies

Toxicity (LD_{50}: average lethal dose at 50% survival) of the studied complexes was determined in albino mice of either gender (body weight 20–25 g). The test compound was injected intraperitoneally at different dose levels in groups of ten animals and per cent mortality in each group was observed after 24 h of drug administration. The LD_{50} value (mg/kg) was calculated from the data according to the procedure reported previously [22–24,28]. The anti-inflammatory activity (% inhibition) of the synthesized derivatives were carried out *in vivo* using the carrageenan-induced paw edema bioassay in rats according to the procedures reported recently [22–24,28].

2.4. Synthesis

Schiff base (H_3L) derived from the condensation of tris(2-aminoethyl)amine and 4-methyl-5-imidazolecarboxaldehyde) was prepared by the reported method [9], and its di- and triorganotin(IV) complexes were synthesized as described below.

2.4.1. Synthesis of Schiff base [tren(4-Me-5-ImH)$_3$] (H_3L)

To a methanol (~20 ml) solution of 4-methyl-5-imidazolecarboxaldehyde (0.446 g, 4.05 mmol) was added tris(2-aminoethyl)amine (0.195 g, 1.33 mmol) in 20 ml of methanol with constant stirring. The resulting reaction mixture was refluxed for 1 h to give yellow solution. The methanol was allowed to evaporate. The resulting yellowish-orange solid of Schiff base (tren(4-Me-5-ImH)$_3$ or H_3L) as shown in Fig. 1 was obtained. It was recrystallized with methanol and dried in vacuum [9].

*2.4.1.1. H_3L (**1**).* Yellowish-orange solid; m.p., 188–190 °C; yield, 80%; *Anal.* Calc. for $C_{21}H_{30}N_{10}$ (422.54): C, 59.69; H, 7.16; N, 33.15. Found: C, 59.61; H, 7.19; N, 33.11%. Selected IR data (KBr, ν_{max}/cm^{-1}): 1646vs ν(C=N)$_{azomethine}$, 1580w, 1486m ν(C=N)$_{ring}$, 1386s δ(N–H)$_{imidazole}$. UV spectral bands, transition, λ_{max} in nm, ε in M^{-1} cm^{-1}: $\pi \rightarrow \pi^*$, 204, 17066; $n \rightarrow \pi^*$, 263, 35958.

2.4.2. Synthesis of diorganotin(IV) complexes of H_3L by the deprotonation with triethylamine

A mixture of 4-methyl-5-imidazolecarboxaldehyde (0.4998 g, 4.5 mmol) and tris(2-aminoethyl)amine (0.2194 g, 1.5 mmol) in 40 ml of methanol in a two neck flask was stirred under inert atmosphere of dry nitrogen and refluxed for 1 h to give a yellow solution. After cooling to room temperature, a methanol solution (~10 ml) of R'_2SnCl_2 (1.5 mmol) and a methanol (~10 ml) solution of triethylamine (0.42 ml, 3.0 mmol), were simultaneously added with constant stirring. It was further stirred for 30–35 h at room temperature. It was centrifuged and filtered in order to remove triethylamine hydrochloride. The excess of solvent was gradually removed by evaporation under reduced pressure. The solid thus obtained was recrystallized from dichloromethane–methanol (2:1 v/v) mixture.

2.4.3. Synthesis of triorganotin(IV) complexes of H_3L by the deprotonation with triethylamine

The procedure for triorganotin(IV) complexes is similar to that of diorganotin(IV) complexes as mentioned in Section 2.4.2. A yellow solution of Schiff base was prepared *in situ* as mentioned in Section 2.4.2. After cooling to room temperature, a methanol solution (~10 ml) of R_3SnCl (1.5 mmol) and a methanol (~10 ml) solution of triethylamine (0.21 ml, 1.5 mmol) were simultaneously added with constant stirring. Rest of the procedure for isolation and recrystallization is the same as mentioned in Section 2.4.2.

*2.4.3.1. $Me_2Sn(HL)$ (**2**).* Orange solid; m.p., 178–180 °C; yield, 94%; *Anal.* Calc. for $C_{23}H_{34}N_{10}Sn$ (569.30): C, 48.53; H, 6.02; N, 24.60, Sn, 20.85. Found: C, 48.49; H, 5.96; N, 24.57, Sn, 20.30%. Selected IR data (KBr, ν_{max}/cm^{-1}): 1639vs ν(C=N)$_{azomethine}$, 1523w, 1452s ν(C=N)$_{ring}$, 1354s δ(N–H)$_{imidazole}$, 637m ν_{as}(Sn–C), 574m ν_s(Sn–C), 452m ν(Sn–N), 424w ν(Sn ← N). UV spectral bands, transition, λ_{max} in nm, ε in $M^{-1}\,cm^{-1}$: $\pi \rightarrow \pi^*$, 207, 18116; $n \rightarrow \pi^*$, 271, 38762.

*2.4.3.2. $Me_3Sn(H_2L)$ (**3**).* Reddish-orange solid; m.p., 138–140 °C; yield, 86%; *Anal.* Calc. for $C_{24}H_{38}N_{10}Sn$ (585.34): C, 49.25; H, 6.54; N, 23.93, Sn, 20.28. Found: C, 49.24; H, 6.55; N, 23.86, Sn, 19.79%. Selected IR data (KBr, ν_{max}/cm^{-1}): 1645vs ν(C=N)$_{azomethine}$, 1513w, 1450m ν(C=N)$_{ring}$, 1352m δ(N–H)$_{imidazole}$, 637m ν_{as}(Sn–C), 573m ν_s(Sn–C), 449m ν(Sn–N), 428w ν(Sn ← N). UV spectral bands, transition, λ_{max} in nm, ε in $M^{-1}\,cm^{-1}$: $\pi \rightarrow \pi^*$, 205, 18790; $n \rightarrow \pi^*$, 267, 37470.

*2.4.3.3. $n\text{-}Pr_3Sn(H_2L)$ (**4**).* Yellow solid; m.p., 110–112 °C; yield, 82%; *Anal.* Calc. for $C_{30}H_{50}N_{10}Sn$ (669.51): C, 53.82; H, 7.53; N, 20.92, Sn, 17.73. Found: C, 53.80; H, 7.48; N, 20.89; Sn, 17.47%. Selected IR data (KBr, ν_{max}/cm^{-1}): 1642vs, 1618s ν(C=N)$_{azomethine}$, 1544sh, 1465m ν(C=N)$_{ring}$, 1348s δ(N–H)$_{imidazole}$, 560w ν_{as}(Sn–C), 501m ν_s(Sn–C), 450w ν(Sn–N), 420m ν(Sn ← N). UV spectral bands, transition, λ_{max} in nm, ε in $M^{-1}\,cm^{-1}$: $\pi \rightarrow \pi^*$, 204, 11116; $n \rightarrow \pi^*$, 270, 17504.

*2.4.3.4. $n\text{-}Bu_2Sn(HL)$ (**5**).* Orange solid; m.p., 135–137 °C; yield, 90%; *Anal.* Calc. for $C_{29}H_{46}N_{10}Sn$ (653.46): C, 53.30; H, 7.10; N, 21.44; Sn, 18.17. Found: C, 53.27; H, 7.11; N, 21.45; Sn, 18.01%. Selected IR data (KBr, ν_{max}/cm^{-1}): 1639vs ν(C=N)$_{azomethine}$, 1516w, 1458m ν(C=N)$_{ring}$, 1352sh δ(N–H)$_{imidazole}$, 630m ν_{as}(Sn–C), 559m ν_s(Sn–C), 448w ν(Sn–N), 418w ν(Sn ← N). UV spectral bands, transition, λ_{max} in nm, ε in $M^{-1}\,cm^{-1}$: $\pi \rightarrow \pi^*$, 204, 13334; $n \rightarrow \pi^*$, 269, 21646.

*2.4.3.5. $n\text{-}Bu_3Sn(H_2L)$ (**6**).* Reddish-orange semi-solid; yield, 87%; *Anal.* Calc. for $C_{33}H_{56}N_{10}Sn$ (711.59): C, 55.70; H, 7.93; N, 19.68; Sn, 16.68. Found: C, 55.67; H, 7.95; N, 19.59; Sn, 16.49%. Selected IR data (KBr, ν_{max}/cm^{-1}): 1642vs ν(C=N)$_{azomethine}$, 1532w, 1462s ν(C=N)$_{ring}$, 1374m δ(N–H)$_{imidazole}$, 633m ν_{as}(Sn–C), 604w ν_s(Sn–C), 453m ν(Sn–N), 420w ν(Sn ← N). UV spectral bands, transition, λ_{max} in nm, ε in $M^{-1}\,cm^{-1}$: $\pi \rightarrow \pi^*$, 205, 20988; $n \rightarrow \pi^*$, 265, 31640.

*2.4.3.6. $Ph_2Sn(HL)$ (**7**).* Orange solid; m.p., 250–252 °C; yield, 88%; *Anal.* Calc. for $C_{33}H_{38}N_{10}Sn$ (693.44): C, 57.16; H, 5.52; N, 20.20; Sn, 17.12. Found: C, 57.10; H, 5.51; N, 20.10; Sn, 16.96%. Selected IR data (KBr, ν_{max}/cm^{-1}): 1643vs ν(C=N)$_{azomethine}$, 1548w, 1466m ν(C=N)$_{ring}$, 1347w δ(N–H)$_{imidazole}$, 280s ν_{as}(Sn–C), 246s ν_s(Sn–C), 460m ν(Sn–N), 424w ν(Sn ← N). UV spectral bands, transition, λ_{max} in nm, ε in $M^{-1}\,cm^{-1}$: $\pi \rightarrow \pi^*$, 207, 24280; $n \rightarrow \pi^*$, 269, 18304.

*2.4.3.7. $Ph_3Sn(H_2L)$ (**8**).* Reddish-orange solid; m.p., 146–148 °C; yield, 91%; *Anal.* Calc. for $C_{39}H_{44}N_{10}Sn$ (771.56): C, 60.71; H, 5.57; N, 18.15; Sn, 15.39. Found: C, 60.67; H, 5.55; N, 18.11; Sn, 15.23%. Selected IR data (KBr, ν_{max}/cm^{-1}): 1640s ν(C=N)$_{azomethine}$, 1515sh, 1462w ν(C=N)$_{ring}$, 1348s δ(N–H)$_{imidazole}$, 280s ν_{as}(Sn–C), 226s ν_s(Sn–C), 456m ν(Sn–N), 413w ν(Sn ← N). UV spectral bands, transition, λ_{max} in nm, ε in $M^{-1}\,cm^{-1}$: $\pi \rightarrow \pi^*$, 207 (25958); $n \rightarrow \pi^*$, 264 (16666).

2.4.4. Synthesis of di-n-octyltin(IV) complex of H_3L by azeotropic removal of water method

To the cooled methanol solution of the pre-prepared Schiff base as described in Section 2.4.2, a hot methanol solution of $n\text{-}Oct_2SnO$ (0.4517 g, 1.5 mmol) was added with constant stirring at room temperature under inert atmosphere of dry nitrogen. The reaction mixture was heated with constant stirring for another ~48 h at 60–65 °C. The solution was filtered to remove unreacted reactants, and the excess of solvent was gradually removed by evaporation under vacuum. The solid thus obtained was recrystallized from dichloromethane–methanol (2:1 v/v) mixture.

2.4.4.1. $n\text{-}Oct_2Sn(HL)$ (9). Reddish-orange solid; m.p., 100–102 °C; yield, 88%; *Anal.* Calc. for $C_{37}H_{62}N_{10}Sn$ (765.68): C, 58.04; H, 8.16; N, 18.29; Sn, 15.50. Found: C, 58.00; H, 8.19; N, 18.25; Sn, 15.52%. Selected IR data (KBr, ν_{max}/cm^{-1}): 1640vs ν(C=N)$_{azomethine}$, 1550m, 1465m ν(C=N)$_{ring}$, 1368m δ(N–H)$_{imidazole}$, 575w ν_{as}(Sn–C), 514w ν_s(Sn–C), 449w ν(Sn–N), 420w ν(Sn ← N). UV spectral bands, transition, λ_{max} in nm, ε in $M^{-1}\,cm^{-1}$: $\pi \rightarrow \pi^*$, 205, 19680; $n \rightarrow \pi^*$, 266, 32762.

Note: vs: very strong; s: strong; m: medium; w: weak; br: broad; sh: shoulder.

3. Results and discussion

3.1. Synthesis, reactivity and solid-state characteristics

The reactions of R_3SnCl and R'_2SnCl_2 with Schiff base (tren(4-Me-5-ImH)$_3$) (H_3L) (formed *in situ*) in a 1:1 M ratio in the presence of Et_3N, led to the formation of the complexes according to Eqs. (1) and (2). The reaction of di-*n*-octyltin(IV) oxide with H_3L (formed *in situ*) in a 1:1 M ratio resulted the product with an azeotropic removal of water according to Eq. (3).

$$H_3L + R_3SnCl + Et_3N \xrightarrow[\text{Room temperature}]{CH_3OH} R_3Sn(H_2L) + Et_3N\cdot HCl \quad (R = Me, n\text{-}Pr, n\text{-}Bu \text{ and } Ph) \tag{1}$$

$$H_3L + R'_2SnCl_2 + 2Et_3N \xrightarrow[\text{Room temperature}]{CH_3OH} R'_2SnCl(HL) + 2Et_3N\cdot HCl \quad (R' = Me, n\text{-}Bu \text{ and } Ph) \tag{2}$$

$$H_3L + n\text{-}Oct_2SnO \xrightarrow[\text{Reflux}]{CH_3OH} Oct_2Sn(HL) + H_2O \tag{3}$$

The above reactions were found to be feasible and required 30–35 h of stirring at room temperature, except the reaction mentioned in Eq. (3), which required ~48 h of stirring at 60–65 °C. All of the synthesized organotin(IV) complexes of H_3L are yellow to orange powder except $n\text{-}Bu_3Sn(H_2L)$, which is semi-solid. The synthesized complexes are obtained in good yield (82–94%) and are hygroscopic in air atmosphere. Diorganotin(IV) and triorganotin(IV) derivatives of H_3L are soluble in methanol and dimethylsulfoxide and have poor solubility in ethanol and other organic solvents. The analytical data of the synthesized complexes are given in Section 2, which show a 1:1 metal-to-ligand ratio. The molar conductance values (at room temperature) of 10^{-3} M solutions (in methanol) of the synthesized organotin(IV) complexes are in the range 5.0–12.0 $ohm^{-1}\,cm^2\,mol^{-1}$, suggesting their non-electrolytic nature.

3.2. Infrared and far-infrared spectral studies

The characteristic infrared and far-infrared frequencies and their assignments in H_3L and its di- and triorganotin(IV) complexes are given in Section 2. Two strong bands observed in the IR spectrum of the ligand at 1580 and 1386 cm^{-1}, which may be assigned to the combination bands (δ(NH)(minor) + ν(C=N)(major)] and (δ(NH)(major) + ν(C=N) (minor)] [31], respectively, are shifted towards lower wave numbers (1550–1513 and 1374–1347 cm^{-1}) in the organotin(IV) complexes, indicating the coordination of ring nitrogen to the central tin atom. The shifts observed in the other bands of imidazole ring in this region are in agreement with structural changes occurring in the ring on account of bonding of ring nitrogen to tin [32].

The IR spectrum of H_3L shows a very sharp and strong band at 1646 cm^{-1} assignable to the ν(C=N) azomethine [33]. In the IR spectra of di- and triorganotin(IV) complexes, the ν(C=N) is slightly shifted to lower wave numbers indicating the coordination of azomethine nitrogen to tin. A slight shift in ν(C=N) azomethine further suggests that all azomethine nitrogens are not taking part in the bonding with central tin atom. The above modes of coordination of H_3L are further supported by the appearance of two new bands at 454 ± 6 and 421 ± 8 cm^{-1} in the spectra of organotin(IV) complexes, which are assigned to ν(Sn–N) [32,33] and ν(Sn ← N) [17], respectively.

The IR and far-IR spectra of di- and trialkyltin(IV) complexes depict two bands at 599 ± 39 and 553 ± 52 cm^{-1} assignable to the ν_{as}(Sn–C) and ν_s(Sn–C), respectively, whereas the corresponding vibrational bands in di- and triphenyltin(IV) analogues are observed at 280 and 236 ± 10 cm^{-1}, respectively [22–28,34]. These data clearly indicate the existence of *c*is-R_3Sn(IV) and R_2Sn(IV) moieties in the studied complexes.

3.3. ^{119}Sn Mössbauer spectrum

The ^{119}Sn Mössbauer spectrum of $Me_3Sn(H_2L)$ could be taken as representative for the assignment of structure of the studied triorganotin(IV) complexes of H_3L. The ^{119}Sn Mössbauer spectrum of $Me_3Sn(H_2L)$ exhibits isomer shift (I.S.) at 0.91 mm s^{-1} and quadrupole splitting (Q.S.) at 3.52 mm s^{-1} showing that the electric field gradient around tin nucleus is produced by the inequalities in the tin–nitrogen bonds and is also due to geometric distortions. The ρ (Q.S./I.S.) value of 3.87 clearly indicates a coordination number greater than four in the solid-state. The observed Q.S. (3.52 mm s^{-1}) and I.S. (0.91 mm s^{-1}) values of $Me_3Sn(H_2L)$ suggested the existence of *fac-cis*-R_3Sn(IV) moieties in a distorted octahedral arrangement around tin atom for the complexes $R_3Sn(H_2L)$ (R = Me, *n*-Pr, *n*-Bu and Ph) (Fig. 2). The gross distortions in octahedral structure may be due to the asymmetry of multidentate ligand (tripodal Schiff base) with different N donor atoms. A similar structure has been reported for the closely related compounds $R_3SnCl{\cdot}L$ (where R = CH_3 and Ph; L = Schiff bases derived from 2-amino-5-(*o*-methoxyphenyl)-1,3,4-thiadiazole) [35].

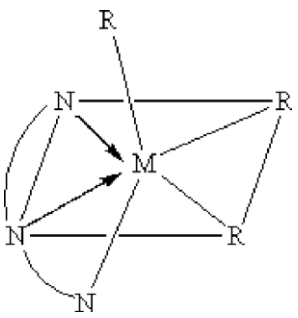

Fig. 2. *fac-cis*-Octahedral structure of $R_3Sn(H_2L)$.

3.4. Electronic spectral studies

In the electronic spectra of Schiff base (H_3L) and its organotin(IV) complexes in methanol, two intense bands are observed at 205 ± 2 and 267 ± 4, which may be due to a $\pi \rightarrow \pi^*$ transition of the imidazole ring and a $n \rightarrow \pi^*$ transition of an >C=N (azomethine) chromophore, respectively. The broad bands obtained in the region 322–329 nm in the spectra of the complexes may be assigned to the charge transfer bands coupled with secondary band of imidazole ring.

3.5. Multinuclear (^{1}H, ^{13}C and ^{119}Sn) NMR spectral studies

3.5.1. ^{1}H NMR spectra

^{1}H NMR spectral data of Schiff base (H_3L) and its di- and triorganotin(IV) complexes are presented in Table 1. In the ^{1}H NMR spectrum of H_3L, a resonance at δ 8.23 ppm has been assigned to the azomethine (–CH=N–) protons. In most of the studied organotin(IV) complexes, three signals are observed in the range δ 8.87–7.33 ppm for azomethine protons, indicating the non-equivalence of azomethine protons. Further, a large shift is observed in two signals ($\Delta\delta$ (0.64–0.05) and (0.24–0.04) ppm, for azomethine protons) in most of the organotin(IV) complexes, suggest the participation of two azomethine nitrogen in coordination. The proton signals of three (–N–CH_2–CH_2–N=) groups (at position 2–3, 2′–3′ and 2″–3″) appear as a broad singlet at δ 3.70 ppm and a multiplet centered at δ 2.86 ppm in H_3L. In the organotin(IV) complexes, a number of resonances with large downfield shift are observed for these protons (see Table 1) which also support the participation of the azomethine nitrogen in bonding to tin.

The exchangeable NH imidazole proton was not observed up to δ 15 ppm under experimental condition in both H_3L and its organotin(IV) complexes [9]. The imidazole protons $(=C–H)_{imidazole}$ of Schiff base appear as a sharp singlet at δ 7.62 ppm, whereas in organotin(IV) complexes, the corresponding protons appear as a number of signals, indicating non-equivalence of imidazole rings. The methyl protons attached to the imidazole ring of H_3L appear as a sharp singlet at δ 2.32 ppm. In most of the studied organotin(IV) complexes, these methyl protons are observed as more than one signals with downfield shift. The shifting observed in the $(=C–H)_{imidazole}$ and $–CH_3$ indicates the participation of imidazole ring nitrogen in coordination. $Ph_2Sn(HL)$ shows more than one resonances for H_γ and H_δ, and one broad doublet for H_β protons of $Sn–C_6H_5$ indicating the presence of more than one tin species in solution. The characteristic signals of all the magnetically non-equivalent alkyl- or phenyl-protons of organotin(IV) moieties have also been assigned, which are in good agreement with reported values [22–28,34].

The $^2J(^1H–^{119/117}Sn)$ coupling constant, which gives important information about the coordination environment, is also determined for some of the organotin(IV) complexes as shown in Table 1. The $^2J(^1H–^{119}Sn)$ values are 76.0 and 80.0 Hz for $Me_2Sn(HL)$, 72.3 and 77.7 Hz for $Me_3Sn(H_2L)$ and 84.8 Hz for *n*-$Bu_3Sn(HL)$ and $^3J(^1H–^{119}Sn)$ for $Ph_2Sn(HL)$ is 75.7 Hz, which lie in the range of a distorted octahedral arrangement [36,37]. In the studied complexes, the values of ∠C–Sn–C calculated by using Lockhart and Manders [36,37] equation ($\theta = 0.0161\ |^2J|^2 - 1.32\ |^2J| + 133.4$) are in the range 122.13–137.18° (Table 1), which also indicates *cis*-organic group in a distorted octahedral geometry around tin.

The number of protons for various groups calculated from the integration curves and from the expected molecular formula are in good agreement with each other.

Table 1
^{1}H NMR spectral data [δ (ppm)] of di- and triorganotin(IV) complexes of H_3L[a].

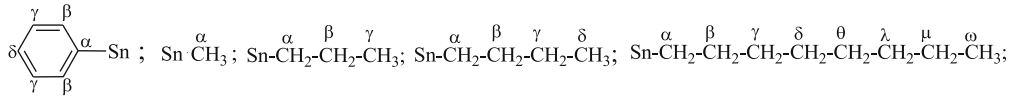

S. No.[b]	δ (H–C=N) (imine)	δ (–CH) (imidazole)	δ (N–CH_2–CH_2–N)	δ (–CH_3)	δ (Sn–R)
1	8.23, s, (3H) [H-5, H-5', H-5"]	7.62, s, (3H) [H-8, H-8', H-8"]	3.67, sbr, (6H); 2.93–2.79, m, (6H)	2.32, s, (9H) [H-11, H-11', H-11"]	
2	8.87, s, (1H); 8.47, s, (1H); 8.39, s, (1H), [H-5, H-5', H-5"]	7.80, s, (1H); 7.69, s, (2H); [H-8, H-8', H-8"]	4.34–4.29, t, 14 Hz, (2H); 4.00–3.93, m, (4H); 3.81, dbr, (2H); 3.22, dbr, (2H); 3.08–3.05, t, (2H)	2.58, s, (6H); 2.45, s, (3H); [H-11, H-11', H-11"]	Hα: 0.94, s, (3H), $^2J(^1H–^{119}Sn)$ [76.0 Hz]; 0.80, s, (3H), $^2J(^1H–^{119}Sn)$ [80.0 Hz]; [C–Sn–C = 126.07°/130.84°][c]
3	7.94, s, (1H); 7.49, s, (1H); 7.33, s, (1H), [H-5, H-5', H-5"]	6.93, s, (1H); 6.82, s, (2H); [H-8, H-8', H-8"]	2.88, dbr, (4H); 2.56–2.52, m, (2H); 2.16, dbr, (6H)	1.71, s, (3H); 1.53, s, (6H); [H-11, H-11', H-11"]	Hα: -0.35, s, (6H), $^2J(^1H–^{119}Sn)$ [72.3 Hz]; −0.36, s, (3H), $^2J(^1H–^{119}Sn)$ [77.7 Hz]; [C–Sn–C = 122.13°/128.06°][c]
4	8.53, s, (1H); 8.40, s, (1H); 8.24, s, (1H), [H-5, H-5', H-5"]	7.78, s, (2H); 7.65, 7.62, d, (1H) [H-8, H-8', H-8"]	4.10, sbr, (2H); 3.87–3.80, sbr, (2H); 3.68–3.64, m, (2H); 3.48, sbr, (2H); 3.23, sbr, (2H); 2.94–2.78, m, (2H)	2.41, s, (6H); 2.35, 2.33, d, (3H); [H-11, H-11', H-11"]	Hα and Hβ: 1.27–0.98, mbr, (12H); H_γ: 0.83–0.82, d, (9H)
5	8.82, s, (1H); 8.45, s, (1H); 8.26, s, (1H), [H-5, H-5', H-5"]	7.72, s, (1H); 7.67, s, (2H); [H-8, H-8', H-8"]	4.28–4.22, t, 14 Hz, (2H); 3.95–3.85, m, (2H); 3.69, dbr, (2H); 3.37–3.31, m, (4H); 3.01–2.96, m, (2H)	2.54, s, (6H); 2.44, s, (3H); [H-11, H-11', H-11"]	Hα: 1.07–1.04, m, (4H); Hβ: 1.45, m, (4H); H_γ: 1.34–1.27, m, (4H); Hδ: 0.66–0.64, t, (3H); 0.95–0.92, t, (3H)
6	8.29, 8.28, d, 5 Hz, (3H) [H-5, H-5', H-5"]	7.75, s, (1H); 7.63, s, (2H); [H-8, H-8', H-8"]	3.69, dbr, (6H); 3.02–2.93, m, (6H)	2.34, s, (6H); 2.54, s, (3H); [H-11, H-11', H-11"]	Hα: 1.22–1.19, t, 8.0 Hz, (6H), $^2J(^1H–^{119}Sn)$ [84.8 Hz]; Hβ: 1.69–1.63, m, (6H), $^3J(^1H–^{119}Sn)$ [59.3 Hz]; H_γ: 1.41–1.35, m, (6H); Hδ: 0.96–0.93, t, 7.5 Hz, (9H); [C–Sn–C = 137.18°][c]
7	8.30, s, (1H); 8.09, s, (1H); 7.97, s, (1H), [H-5, H-5', H-5"]	7.77, s, (1H); 7.68, s, (1H); 7.66, s, (1H); [H-8, H-8', H-8"]	4.33–4.27, t, (4H); 4.13–4.10, t, (4H); 3.71–3.69, t, (2H); 3.51–3.48, t, (2H);	2.54, s, (3H); 2.34, s, (3H); 2.28, s, (3H); [H-11, H-11', H-11"]	Hβ: 7.82, d br, 3.5 Hz, (4H), $^3J(^1H–^{119}Sn)$ [75.7 Hz]; H_γ: 7.29–7.26, m, (2H), 7.23, sbr, (2H), $^4J(^1H–^{119}Sn)$ [83.7 Hz]; Hδ: 7.43–7.42, t, (1H), 7.39–7.38, t, (1H), $^5J(^1H–^{119}Sn)$ [43.9 Hz]
8	8.30, s, (1H); 8.27, s, (1H); 8.15, s, (1H), [H-5, H-5', H-5"]	7.33, d, (1H); 7.23–7.19, dd, (2H); [H-8, H-8', H-8"]	3.58, dbr, (6H); 2.99, 2.78, sbr, (6H)	2.49, s, (3H); 2.32, s, (6H); [H-11, H-11', H-11"]	Hβ: 7.76, dbr, (6H), $^3J(^1H–^{119}Sn)$ [72.5 Hz]; H_γ: 7.46–7.43, t, 7.0 Hz, (6H); Hδ: 7.57, dbr, (3H)
9	8.30, s, (1H); 8.28, s, (2H), [H-5, H-5', H-5"]	7.75, s, (1H); 7.63, s, (2H) [H-8, H-8', H-8"]	3.69, dbr, (6H); 3.02–2.93, m, (6H)	2.49, s, (3H); 2.34, s, (6H); [H-11, H-11', H-11"]	Hα-μ[d]: 1.76–1.68, 1.21–1.18, m, (28H); Hω:1.04–1.01, t, 7.0 Hz, (6H)

[a] Hydrogen number as indicated in Fig. 1 of H_3L.
[b] S.no. as indicated in Section 2; s: singlet; d: doublet; dd: double doublet; t: triplet; m: multiplet; br: broad; sbr, singletbroad, dbr, doubletbroad, mbr, multipletbroad.
[c] Calculated using Eq. ($\theta = 0.0161\ |^2J|^2 - 1.32\ |^2J| + 133.4$).
[d] Strongly overlapping multiplets.

3.5.2. ^{13}C NMR spectra

The ^{13}C NMR spectral data along with assignment of characteristic peaks of H_3L and its di- and triorganotin(IV) complexes are presented in Table 2. In the ^{13}C NMR spectrum of H_3L, carbons attached to three azomethine nitrogens, viz. C-5, C-5′ and C-5″ are observed at δ 152.86 ppm [33]. However, in all of the studied organotin(IV) complexes, two or three resonances due to azomethine carbons are observed indicating the non-equivalence of these groups. Further, in the ^{13}C NMR spectra of organotin(IV) complexes, the signals of C(8, 8′), C(10, 10′), C(6, 6′) and methyl groups (C-11, 11′) are shifted to downfield 137.04 ± 1.17, 129.75 ± 1.61, 140.83 ± 3.68 and 12.14 ± 3.45 ppm, respectively, as expected for a process involving deprotonation of N(9)–H for triorganotin(IV) derivatives and N(9)–H and N(9′)–H for diorganotin(IV) derivatives. The alkyl carbons of Schiff base and organotin(IV) complexes appear well within the expected ranges and their assignment are given in Table 2. All the magnetically non-equivalent carbons of alkyl- or phenyl- groups attached to tin are identified and their chemical shift values are in close agreement with reported values [34]. Moreover, presence of more than one signal for tin–phenyl carbons for $Ph_2Sn(HL)$ (Table 2) also suggests that these groups are present in magnetically different environments of more than one tin species in solution.

The heteronuclear coupling constant $^1J(^{13}C–^{119}Sn)$ in the studied organotin(IV) complexes are determined, which provide vital information about the coordination environment and geometry of the complexes. In all the complexes, the satellite are resolved and observed $^1J(^{13}C–^{119}Sn)$ values are in the range 690.56–759.86 Hz as given in Table 2.

These values lie in a typical range for six-coordinated organotin(IV) complexes [36–38]. Moreover, the calculated values of ∠C–Sn–C using observed $^1J(^{13}C–^{119}Sn)$ values in the equation given by Lockhart and Manders [36,37] ($|^2J| = 11.4\theta - 875$) are in the range of 137.3–143.4° (as given in Table 2), which are intermediate between the corresponding values for *cis*-octahedral (∠C–Sn–C = 90°) and *trans*-octahedral (∠C–Sn–C = 180°) organotin(IV) moieties. Thus, the most plausible structure of these complexes is best described by a highly distorted octahedral geometry with *cis*-organic groups [31].

3.5.3. ^{119}Sn NMR spectra

The ^{119}Sn NMR spectral data of organotin(IV) derivatives of H_3L are given in Table 3. The ^{119}Sn NMR spectrum of $Ph_2Sn(HL)$ is shown in Fig. 3. The ^{119}Sn NMR chemical shifts are very sensitive to coordination number of tin and are greatly shifted upfield up on coordination to Lewis base. Typical ranges of ^{119}Sn chemical shifts have been reported [39] for coordination number five (δ −90 to −330 ppm) and six (δ −125 to −515 ppm) organotin(IV) complexes in $CDCl_3$ solution. The ^{119}Sn spectra of the studied di- and triorganotin(IV) complexes, except $Ph_2Sn(HL)$, exhibit only

Table 2
^{13}C NMR spectral data of the di- and triorganotin(IV) complexes of H_3L[a,b] in CD_3OD.

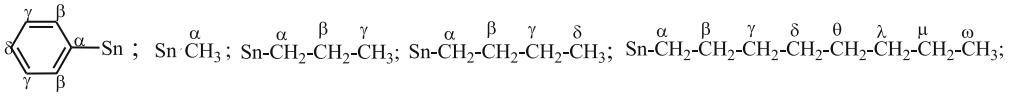

Ligand/ complex[c]	δ (ppm)
1	C-5, C-5′, C-5″: 152.86; C-6, C-6′, C-6″: 137.59; C-8, C-8′, C-8″: 136.39, 136.65; C-10, C-10′, C-10″: 128.08; C-3, C-3′, C-3″: 58.67; C-2, C-2′, C-2″: 55.34, 55.01; C-11, C-11′ C-11″: 9.98, 10.20
2	C-5, C-5′, C-5″: 156.52, 154.40; C-6, C-6′, C-6″: 137.19 (137.59)[d]; C-8, C-8′, C-8″: 136.41, 136.03; C-10, C-10′, C-10″: 130.79; C-3, C-3′: 51.40 (50.85)[d]; C-3″: 53.04; C-2, C-2′: 48.49, 48.55; C-2″: 45.45; C-11: 15.58; C-11′: 15.04; C-11″: 9.90; C-α: 8.06 (8.19)[d] [$^1J(^{13}C–^{119}Sn)$ = 701.0 Hz]; [∠C–Sn–C = 138.2°][e]
3	C-5, C-5′, C-5″: 153.64, 153.38; C-6, C-6′, C-6″: 139.50; C-8, C-8′, C-8″: 136.86, 136.25; C-10, C-10′, C-10″: 130.10; C-3, C-3′, C-3″: 58.48 (57.88)[d]; C-2, C-2′, C-2″: 55.02, 51.29; C-11: 13.07; C-11′: 9.95; C-11″: 9.21; C-α: −4.47 [$^1J(^{13}C–^{119}Sn)$ = 690.56 Hz]; [∠C–Sn–C = 137.3°][e]
4	C-5, C-5′, C-5″: 154.21, 153.86, 152.93; C-6, C-6′, C-6″: 144.50, 143.93; C-8, C-8′, C-8″: 136.64, 136.46, 135.87; C-10, C-10′, C-10″: 131.26; 128.82 (128.04)[d]; C-3, C-3′, C-3″: 58.77, 55.40, 55.07; C-2, C-2′, C-2″: 53.14, 52.25, 49.67, 45.45; C-11, C-11′, C-11″: 11.19, 10.30; C-α: 22.29 [$^1J(^{13}C–^{119}Sn)$ = 714.60 Hz]; C-β: 32.53, 31.53, 28.64, 28.52 [$^2J(^{13}C–^{119}Sn)$ = 126.21, 42.91, 106.01 Hz]; C-γ: 13.16; [∠C–Sn–C = 139.4°][e]
5	C-5, C-5′, C-5″: 156.23; C-6, C-6′, C-6″: 139.40; C-8, C-8′, C-8″: 138.20; C-10, C-10′, C-10″: 131.36; C-3, C-3′, C-3″: 51.58; C-2, C-2′, C-2″: 49.01; C-11, C-11′ C-11″: 8.69; C-α: 25.50 [$^1J(^{13}C–^{119}Sn)$ = 729.04 Hz]; C-β: 27.29, [$^2J(^{13}C–^{119/117}Sn)$ = 57.94 Hz]; C-γ: 27.17 [$^3J(^{13}C–^{119}Sn)$ = 82.46 Hz]; C-δ: 13.03, 12.24; [∠C–Sn–C = 140.7°][e]
6	C-5, C-5′,C-5″: 153.57, 153.16; C-6, C-6′, C-6″: 138.02; C-8, C-8′, C-8″: 136.86, 136.25; C-10, C-10′, C-10″: 128.23; C-3″: 58.55, 58.17; C-3, C-3′: 55.23, 55.03; C-2, C-2′ C-2″: 51.42, 48.51; C-11, C-11′, C-11″:10.06, 9.29; C-α: 16.52 [$^1J(^{13}C–^{119}Sn)$ = 729.64 Hz]; C-β: 27.86 [$^2J(^{13}C–^{119}Sn)$ −47.50 Hz]; C-γ: 26.76 [$^3J(^{13}C–^{119}Sn)$ = 70.08 Hz]; C-δ: 12.71 [$^4J(^{13}C–^{119}Sn)$ = 47.39 Hz]; [∠C–Sn–C = 140.8°][e]
7	C-5, C-5′, C-5″: 159.45, 158.39, 154.46; C-6, C-6′, C-6″:137.98, 137.46, 137.15; C-8, C-8′, C-8″: 136.23, 136.05; C-10, C-10′, C-10″: 128.68, 128.14; C-3, C-3′, C-3″: 53.73, 52.39; C-2, C-2′, C-2″: 50.16, 48.54; C-11, C-11′, C-11″: 10.18; 9.90, 8.52; C-α: 146.93, 146.54, 143.99 [$^1J(^{13}C-^{119}Sn)$ = 759.86 Hz]; C-β: 133.19, 132.85, 131.40 [$^2J(^{13}C–^{119}Sn)$ = 123.25 Hz, 110.12 Hz]; C-γ: 129.33, 129.10, 128.83, 128.42 [$^3J(^{13}C-^{119}Sn)$ = 47.02, 38.08, 40.17 Hz]; C-δ: 131.40, 130.64, 130.07 [$^4J(^{13}C–^{119}Sn)$ = 121.14 Hz]; [∠C–Sn–C = 143.4°][e]
8	C-5, C-5′, C-5″: 157.61, 153.61; 153.27; C-6, C-6′, C-6″: 137.49, 137.33; C-8, C-8′, C-8″: 136.56; C-10, C-10′, C-10″: 127.97; C-3, C-3′, C-3″: 58.32, 54.96; C-2, C-2′, C-2″: 51.85, 51.30, 50.18, 48.53; C-11, C-11′, C-11″: 10.28, 10.06, 9.31; C-α: 140.21 [$^1J(^{13}C–^{119}Sn)$ = 725.02 Hz]; C-β: 136.15 [$^2J(^{13}C–^{119}Sn)$ = 43.05 Hz]; C-γ: 128.45 [$^3J(^{13}C–^{119}Sn)$ = 66.12 Hz]; C-δ: 129.24 [$^4J(^{13}C–^{119}Sn)$ = 51.16 Hz]; [∠C–Sn–C = 140.3°][e]
9	C-5, C-5′, C-5″: 155.45, 153.55; 153.13; C-6, C-6′, C-6″: 137.93; C-8, C-8′, C-8″: 136. 89, 136.28; C-10, C-10′, C-10″: 130.05, 128.20; C-3, C-3′, C-3″: 58,57, 58.23, 55.26; C-2, C-2′, C-2″: 55.05, 51.76, 51.53; C-11, C-11′, C-11″: 10.09, 9.77, 9.31; C-α: 19.30 [$^1J(^{13}C–^{119}Sn)$ = 695.95 Hz]; C-β-C-μ: 30.62, 28.90, 20.96, 20.89, 19.18, 19.08, 18.98; C-ω: 17.69 [$^8J(^{13}C-^{119}Sn)$ = 70 Hz]; [∠C–Sn–C = 137.7°][e]

[a] Ref. [9].
[b] Carbon No. as indicate in Fig. 1 of H_3L.
[c] S. No. as indicated in Section 2.
[d] Calculated using Eq.($|^2J| = 11.4\theta - 875$).
[e] Small peak.

Table 3
^{119}Sn NMR spectral data of the synthesized di- and triorganotin(IV) complexes of H_3L.

Complex No.[a]	δ (ppm)
2	−402.09
3	−415.73
4	−421.89
5	−412.53
6	−268.09
7[b]	−523.65, −599.59, −607.24
8	−535.70
9	−420.60

[a] S. No. as indicated in Section 2.
[b] Intensity ratio of the peaks is 7:2:1 respectively.

one signal which rules out the possibility of two different tin species. The observed ^{119}Sn chemical shift values in the range δ −268.09 to −523.65 ppm (Table 3) suggest six-coordination correspond to the octahedral geometry around tin. The spectrum of $Ph_2Sn(HL)$ shows two additional signals at δ −599.50 and −607.24 ppm, which may be due to a complex species with higher coordination number viz., hepta-coordinated tin. This suggests either the presence of two or more types of different tin environments or a fast interchange of two or more different species in the solution. Therefore, ^{119}Sn NMR spectral data of $Ph_2Sn(HL)$ reveal that the weak interactions between central tin with central nitrogen ((N-1) triethylamine) or third azomethine nitrogen may occur or a solvent molecule may occupy seventh coordination site leading to the fast interchange of octahedral species to pentagonal-bipyramidal species in the solution. The intensity ratio of these three peaks is 7:2:1 indicating the hepta-coordinated species are the minor species in solution.

The possible geometries around tin in di- and triorganotin(IV) complexes of H_3L is best described by a *cis*-distorted octahedral or skew trapezoidal-bipyramidal configuration as shown in Figs. 4 and 5, respectively, whereas in $Ph_2Sn(HL)$, structure is described by the interchange of *cis*-distorted octahedral to pentagonal-bipyramidal as shown in Fig. 6a–c.

3.6. Biological studies

3.6.1. Anti-inflammatory activity

The anti-inflammatory activity (% inhibition) data of the synthesized complexes are presented in Table 4. The activity of the standard drug phenylbutazone has been used for comparison. Organotin(IV) complexes of H_3L exhibited anti-inflammatory activity of varying degree (6.38–20.26% inhibition), which are more active than Schiff base (H_3L) (5.21% inhibition). It has also been observed that organotin(IV) complexes show better activity as compared to the starting organotin(IV) chloride/oxides (Table 4) with only exception of Me_3SnCl (9.89% inhibition), which is slightly more active than that of its Schiff base complex, $Me_3Sn(H_2L)$ (8.89% inhibition). Among the studied organotin(IV) derivatives of Schiff base (H_3L), phenyl derivatives are more active than the alkyl analogues. Further, triorganotin(IV) derivatives are found to be more active than diorganotin(IV) analogues, viz. $Me_3Sn(H_2L)$ (8.89% inhibition) > $Me_2Sn(HL)$ (6.38% inhibition), *n*-$Bu_3Sn(H_2L)$ (16.69% inhibition) > *n*-$Bu_2Sn(HL)$ (12.28% inhibition) and $Ph_3Sn(H_2L)$ (20.26%

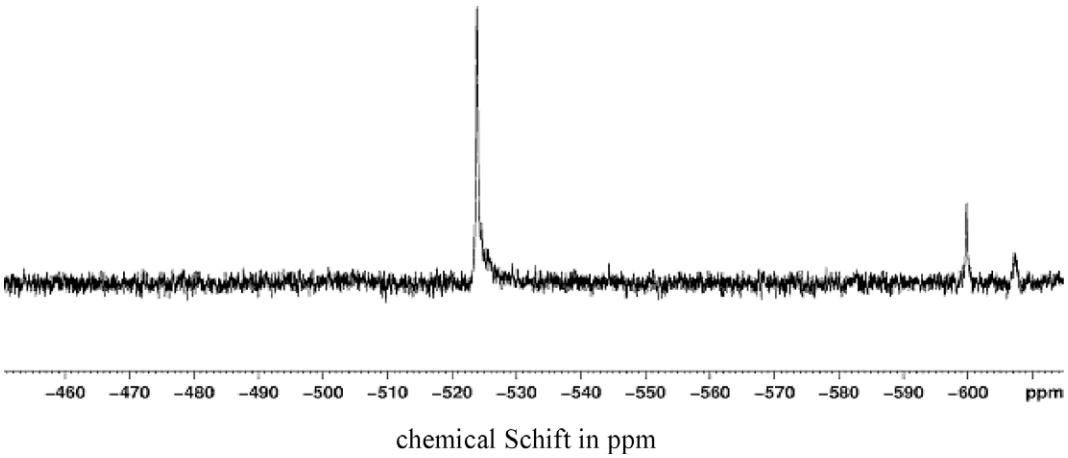

Fig. 3. ^{119}Sn NMR spectrum of $Ph_2Sn(HL)$ (**6**).

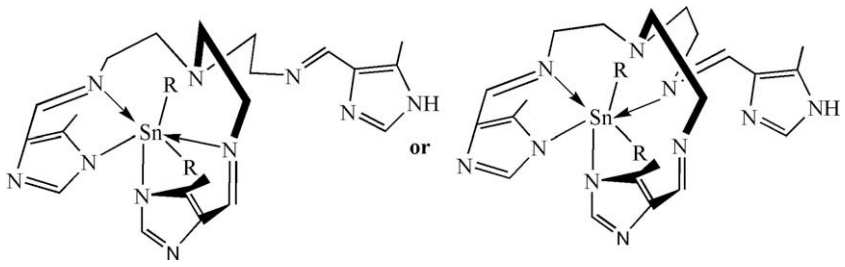

Fig. 4. Plausible distorted *cis*-octahedral structure/skew trapezoidal-bipyramidal configuration of $R_2Sn(HL)$ (R = Me, *n*-Bu, *n*-Oct and Ph).

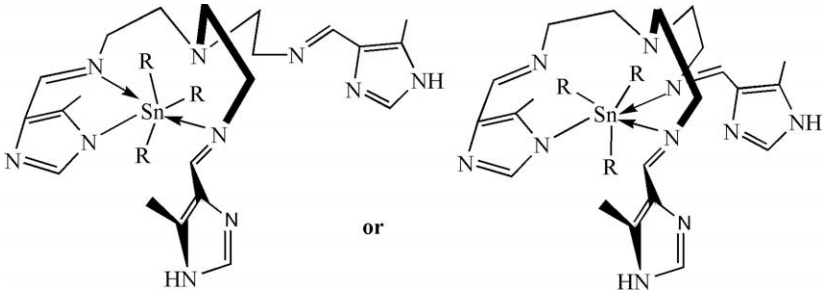

Fig. 5. Plausible distorted *cis*-octahedral structure of $R_3Sn(H_2L)$ (R = Me, *n*-Pr, *n*-Bu and Ph).

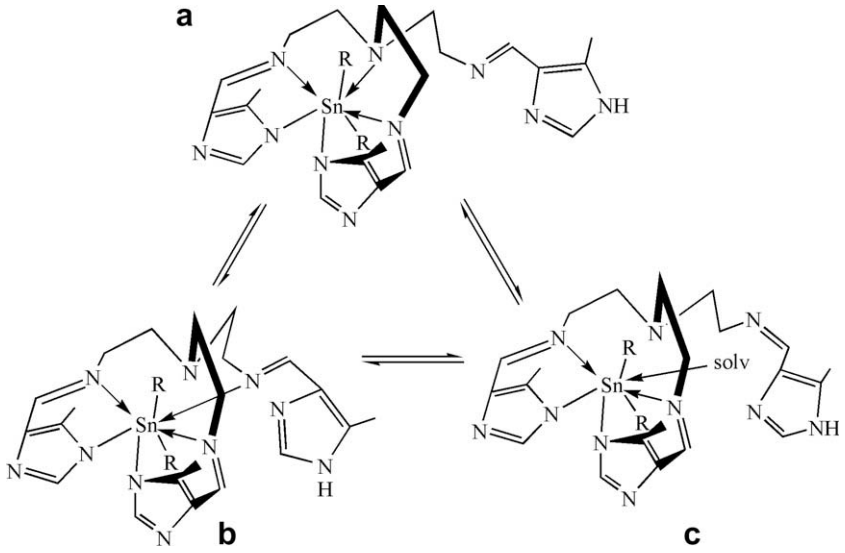

Fig. 6. Plausible interchange of geometry in $Ph_2Sn(HL)$ from distorted octahedral/ pentagonal-bipyramidal geometry through the extra bonding modes of central tin to (a) central N-1 (triethylamine) or (b) third azomethine; or (c) coordination of one solvent molecule.

Table 4
Anti-inflammatory activity and toxicity data of Schiff base (H_3L), organotin(IV) complexes of H_3L, organotin(IV) chlorides/oxides and phenylbutazone.

Complex/starting materials/reference drug	Anti-inflammatory activity		Toxicity LD_{50} (mg/kg p.o.)
	Dose (mg/kg p.o.)	% Oedema inhibition	
H_3L	40	5.21	>400
$Me_2Sn(HL)$	40	6.38	>400
$Me_3Sn(H_2L)$	40	8.89	>400
n-$Bu_2Sn(HL)$	40	12.28	>800
n-$Bu_3Sn(H_2L)$	40	16.69	>800
$Ph_2Sn(HL)$	40	17.78	>800
$Ph_3Sn(H_2L)$	20	10.15	>800
	40	20.26	
	80	36.30	
n-$Oct_2Sn(HL)$	40	9.23	>400
n-$Pr_3Sn(H_2L)$	40	7.17	>400
Me_2SnCl_2	40	2.97	>400
n-Bu_2SnCl_2	40	5.35	>400
Ph_2SnCl_2	40	4.65	>400
n-$(Oct)_2SnO$	40	6.39	>400
Me_3SnCl	40	9.89	>400
n-Pr_3SnCl	40	5.13	>400
n-Bu_3SnCl	40	4.89	>400
Ph_3SnCl	40	7.29	>400
Phenylbutazone	20	12.67	–
	40	31.89	–
	80	48.26	–

inhibition) > $Ph_2Sn(HL)$ (17.78% inhibition), but they are less active than phenylbutazone (31.89% inhibition). Among triorganotin(IV) complexes, the order of their percent inhibition is: n-$Pr_3Sn(H_2L)$ < $Me_3Sn(H_2L)$ < n-$Bu_3Sn(H_2L)$ < $Ph_3Sn(H_2L)$. Furthermore, among diorganotin(IV) complexes, the order of their percent inhibition is $Me_2Sn(HL)$ < n-$Oct_2Sn(HL)$ < n-$Bu_2Sn(HL)$ < $Ph_2Sn(HL)$ as shown in Table 4. The observed activity may be due to the easier formation of Ph_3Sn^{1+}/Ph_2Sn^{2+} moiety. The analysis of data of Table 4 indicates that the anti-inflammatory activity of the studied complexes is influenced by the nature of organic groups attached to tin as well as the coordinating environment of tin.

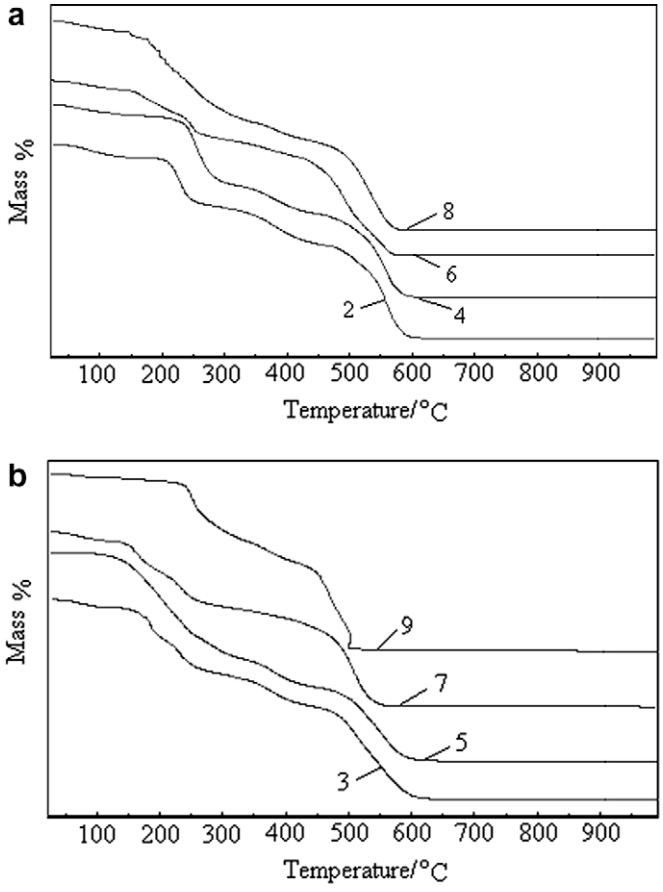

Fig. 7. TGA profiles of (a) $R_2Sn(HL)$ (R = Me, n-Bu, n-Oct and Ph) and (b) $R_3Sn(H_2L)$ (R = Me, n-Pr, n-Bu and Ph).

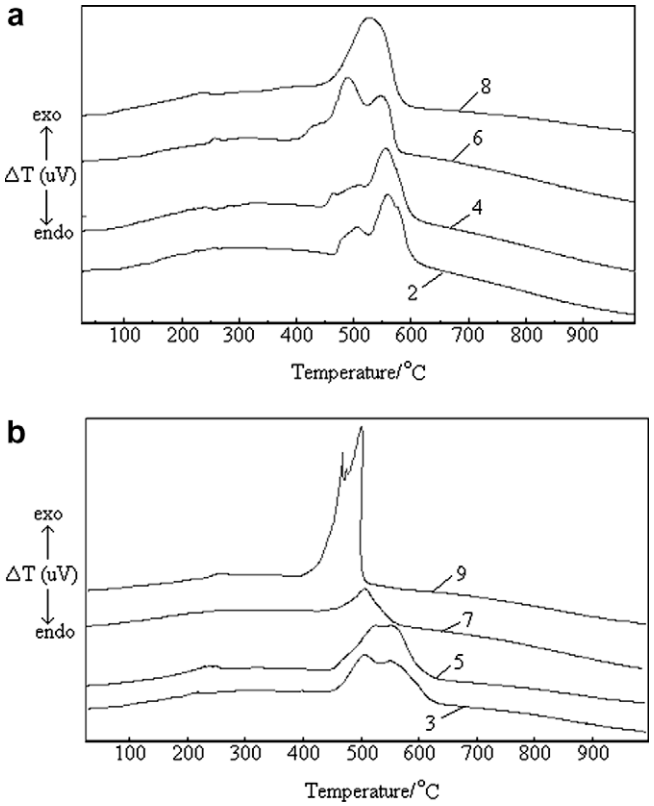

Fig. 8. DTA curves of (a) $R_2Sn(HL)$ (R = Me, n-Bu, n-Oct and Ph) and (b) $R_3Sn(H_2L)$ (R = Me, n-Pr, n-Bu and Ph).

3.6.2. Toxicity studies

The LD_{50} values of the studied complexes are presented in Table 4. All of the complexes have LD_{50} values greater than >400 mg kg^{-1}, suggesting their safety margin. Further, di- and tributyltin(IV) as well as di- and triphenyltin(IV) derivatives showed LD_{50} value (>800 mg kg^{-1}) greater than that of di- and trimethyltin(IV), di-*n*-octyltin(IV) and tri-*n*-propyltin(IV) derivatives (>400 mg kg^{-1}).

Among all of the studied complexes, $Ph_3Sn(H_2L)$ is the most active and has less toxicity.

3.7. Thermal studies

The TG and DTA curves of studied organotin(IV) complexes are presented in Figs. 7 and 8, respectively, and thermal decomposition data are given in Table 5. The main diffraction lines of the residues thus obtained by pyrolysis of the studied organotin(IV) complexes have been summarized in Table 6.

All of the studied organotin(IV) complexes of Schiff base (H_3L) decompose in two steps, except *n*-$Pr_3Sn(H_2L)$, which decomposes in a single step. $Me_2Sn(HL)$ and $Ph_2Sn(HL)$ decompose in a similar manner and mass losses in the first step and second steps are given in Table 5. However, the total observed mass loss in $Me_2Sn(HL)$ is greater than the calculated values (Table 5) due to the partial mass loss through sublimation followed by oxidation to SnO_2, which is evidenced by the exothermic peak at ~550 °C observed in DTA (Table 5 and Fig. 8). The residue of $Me_2Sn(HL)$ left at 610 °C and that of $Ph_2Sn(HL)$ at 570 °C has been analyzed by IR and XRD. The ν(Sn–O) at 617/619 cm^{-1} [34] in IR spectrum of the residue indicated the formation of SnO_2 which was confirmed by its XRD data. The observed *d* values in the residue are in good agreement with the reported values for SnO_2 [40]. *n*-$Bu_2Sn(HL)$ and *n*-$Oct_2Sn(HL)$ show a similar two steps TG profiles (Fig. 7) and mass losses are given in Table 5. The masses of residues left are 11.07% (for SnO_2 calc.: 21.99%) for *n*-$Bu_2Sn(HL)$ and 4.43% (for SnO_2 calc.: 18.89%) for *n*-$Oct_2Sn(HL)$. The main diffraction lines observed in the XRD pattern of the residues are found to correspond to those of SnO_2, which is also supported by the presence of ν(Sn–O) at 618 and 617 cm^{-1}, respectively, in the IR spectra.

Among triorganotin(IV) complexes, $Me_3Sn(H_2L)$ and *n*-$Bu_3Sn(H_2L)$ decompose in two steps, whereas $Ph_3Sn(H_2L)$ and *n*-$Pr_3Sn(H_2L)$ decompose differently. The mass losses in the first step

Table 5
Thermal analysis data of organotin(IV) complexes of Schiff base (H_3L) in air.

Complex	Step no.	Temperature range in TG (°C)	Peak temperature in DTG (°C)	Peak temperature in DTA (°C)	Enthalpy (mJ/mg)	Loss of mass% (obsd.) (calc.)	Species lost
$Me_2Sn(HL)$	I	70–253	230			26.69 (26.56)	$C_8H_{13}N_3$
	II	253–606	505	505 (exothermic)	−1098.7	62.94 (52.59)	$C_{15}H_{21}N_7$ + Sn sublimation and oxidation
			557	560 (exothermic)	−1917.3		
$Me_3Sn(H_2L)$	I	29–439	187			51.32 (51.67)	$C_{16}H_{26}N_6$
	II	439–623	505	508 (exothermic)	−2216.6	41.03 (28.94)	$C_8H_{12}N_4$ + Sn sublimation and oxidation
			549	550 (exothermic)	−1973.4		
n-$Pr_3Sn(H_2L)$	I	199–502	250	258 (exothermic)	−79.3	78.42 (82.12)	$C_{30}H_{49}N_{10}$ + Sn sublimation and oxidation
			462	469 (exothermic)	−2498.7		
			496	500 (exothermic)	−2967.3		
n-$Bu_2Sn(HL)$	I	27–305	259	256 (endothermic)	43.9	37.53 (38.32)	$C_{15}H_{28}N_3$
	II	305–602	551	465 (exothermic)	−655.6	51.40 (43.51)	$C_{14}H_{18}N_7$ + Sn sublimation and oxidation
				509 (exothermic)	−792.9		
				556 (exothermic)	−1448.3		
n-$Bu_3Sn(H_2L)$	I	27–355	198, 224	239 (exothermic)	−210	54.92 (54.32)	$C_{22}H_{38}N_6$
	II	355–601	522	523 (exothermic)	−1972	41.64 (28.99)	$C_{11}H_{18}N_4$ + Sn sublimation and oxidation
			552	551 (exothermic)	−1972		
$Ph_2Sn(HL)$	I	24–380	166, 250	259 (exothermic)	−31.9	31.94 (30.75)	$C_{13}H_{15}N_3$
	II	380–570	442	430 (exothermic)	−913.1	46.32 (52.12)	$C_{20}H_{23}N_7$ + Sn oxidation
			478	488 (exothermic)	−1945.4		
			542	549 (exothermic)	−1528.5		
$Ph_3Sn(H_2L)$	I	28–299	166, 168, 238			34.95 (35.30)	$C_{14}H_{20}N_6$
	II	299–568	505	508 (exothermic)	−2980	46.59 (49.31)	$C_{25}H_{24}N_4$ + Sn oxidation
n-$Oct_2Sn(HL)$	I	25–363	149, 176, 196	233 (exothermic)	−82.9	48.08 (47.35)	$C_{23}H_{44}N_3$
	II	363–571	526	528 (exothermic)	−4238	47.49 (37.14)	$C_{14}H_{18}N_7$ + Sn sublimation and oxidation

Table 6
The main diffraction lines (intensity) for the residue obtained.

Tin compound/residue of complex	Main diffraction lines *d* (Å) (intensity (%)) (*h k l*)				
	1	**2**	**3**	**4**	**5**
Sn[a]	2.92 (100)	2.79 (90)	2.06 (34)	2.02 (74)	1.48 (23)
	(2 0 0)	(1 0 1)	(2 2 0)	(2 1 1)	(1 1 2)
SnO[a]	3.39 (100)	3.00 (50)	2.89 (90)	2.67 (90)	1.77 (80)
SnO_2[a]	3.35 (100)	2.64 (80)	2.37 (25)	1.77 (65)	1.68 (18)
	(1 1 0)	(1 0 1)	(2 0 0)	(2 1 1)	(2 2 0)
$Me_2Sn(HL)$	3.33 (100)	2.63 (98)	2.36 (35)	1.76 (96)	1.67 (24)
$Me_3Sn(H_2L)$	3.34 (94)	2.64 (100)	2.36 (31)	1.76 (67)	1.68 (27)
n-$Pr_3Sn(H_2L)$	3.34 (100)	2.64 (76)	2.37 (32)	1.77 (37)	1.68 (20)
n-$Bu_2Sn(HL)$	3.34 (100)	2.63 (81)	2.36 (39)	1.76 (61)	1.67 (29)
$Ph_2Sn(HL)$	3.32 (37)	2.64 (40)	2.35 (34)	1.73 (19)	1.68 (16)
$Ph_3Sn(H_2L)$	3.35 (100)	2.64 (98)	2.36 (31)	1.76 (92)	1.67 (25)
n-$Oct_2Sn(HL)$	3.34 (100)	2.64 (72)	2.35 (47)	1.76 (51)	1.68 (36)

[a] Ref. [40].

of decomposition are observed, 51.32% (calc.: 51.67%) and 54.92% (calc.: 54.32) corresponding to the loss of $C_{14}H_{20}N_6 + 2CH_3$ for $Me_3Sn(H_2L)$ and $C_{14}H_{20}N_6 + 2C_2H_9$ for n-$Bu_3Sn(H_2L)$, respectively. The remaining organic groups attached to tin and rest part of Schiff base moiety are lost in the second step (Table 5) followed by the sublimation and oxidation of material to SnO_2 [41] which is evidenced by the exothermic peaks observed in DTA (Fig. 8). Further, the XRD analysis of the residue confirms the formation of SnO_2, which is also supported by the ν(Sn–O) observed at 617 cm^{-1} in the IR spectrum.

In $Ph_3Sn(H_2L)$, the mass loss (34.95%) in the temperature range 28–299 °C, corresponds to the loss of Schiff base moiety $C_{14}H_{20}N_6$ (calc.: 35.30%) and the rest of Schiff base moiety ($C_7H_9N_4$) and phenyl groups (3Ph) attached to tin (weight loss: $C_{25}H_{24}N_4$; observed: 46.59%; calculated: 49.31%) are lost in the second step, followed by the oxidation of tin to tin oxide as evidenced by an exothermic peak in DTA curve (Fig. 8). The mass of residue left is 18.45%, which corresponds to SnO_2 (calc.: 18.76%). Whereas the decomposition of n-$Pr_3Sn(H_2L)$ occurs in single step and the experimental mass loss (observed: 78.42%) corresponds to the loss of all organic moieties (calc.: 82.12%) along with oxidation of tin, which is evidenced by an exothermic peak at ~500 °C observed in its DTA. The end product (SnO_2) in both the cases is confirmed by the appearance of ν(Sn–O) at 620 cm^{-1} and observed d values in its XRD spectrum.

Acknowledgements

The authors are thankful to the Head, Institute Instrumentation Centre, Indian Institute of Technology Roorkee, Roorkee, India, for providing facilities to carry out (^{1}H, ^{13}C and ^{119}Sn) NMR measurements, thermal studies, X-ray diffraction analysis. The authors are also grateful to Dr. Dipankar Das, Scientist F, UGC-DAE Consortium for Scientific Research, Kolkata, India, for recording and providing ^{119}Sn Mössbauer spectrum of only one complex. One of the authors (Mr. Pramendra Kumar Saini) is thankful to the Council of Scientific and Industrial Research, New Delhi, India, for awarding Senior Research Fellowship.

References

[1] C.T. Brewer, G. Brewer, M. Shang, W.R. Scheidt, I. Muller, Inorg. Chim. Acta 278 (1998) 197.
[2] Y. Sunatsuki, Y. Ikuta, N. Matsumoto, H. Ohta, M. Kojima, S. Iijima, S. Hayami, Y. Maeda, S. Kaizaki, F. Dahan, J.-P. Tuchagues, Angew. Chem., Int. Ed. 42 (2003) 1614.
[3] F. Lambert, C. Policar, S. Durot, M. Cesario, L. Yuwei, H. Korri-Youssoufi, B. Keita, L. Nadjo, Inorg. Chem. 43 (2004) 4178.
[4] Y. Sunatsuki, M. Sakata, S. Matsuzaki, N. Matsumoto, M. Kojima, Chem. Lett. (2001) 1254.
[5] F. Lambert, J.P. Renault, C. Policar, I. Morgenstern-Badarau, M. Cesario, Chem. Commun. (2000) 35.
[6] C. Brewer, G. Brewer, G. Patil, Y. Sun, C. Viragh, R.J. Butcher, Inorg. Chim. Acta 358 (2005) 3441.
[7] Y. Ikuta, M. Ooidemizu, Y. Yamahata, M. Yamada, S. Osa, N. Matsumoto, S. Iijima, Y. Sunatsuki, M. Kojima, F. Dahan, J.-P. Tuchagues, Inorg. Chem. 42 (2003) 7001.
[8] M. Yamada, M. Ooidemizu, Y. Ikuta, S. Osa, N. Matsumoto, S. Iijima, F. Dahan, J.-P. Tuchagues, Inorg. Chem. 42 (2003) 8406.
[9] C.T. Brewer, G. Brewer, C. Luckett, G.S. Marbury, C. Viragh, A.M. Beatty, W.R. Scheidt, Inorg. Chem. 43 (2004) 2402.
[10] G. Brewer, C. Luckett, L. May, A.M. Beatty, W.R. Scheidt, Inorg. Chim. Acta 357 (2004) 2390.
[11] G. Brewer, C. Luckett, Inorg. Chim. Acta 358 (2005) 239.
[12] G. Brewer, C. Brewer, R.J. Butcher, E.E. Carpenter, Inorg. Chim. Acta 359 (2006) 1263.
[13] L. Tian, Z. Shang, X. Zheng, Y. Sun, Y. Yu, B. Qian, X. Liu, Appl. Organomet. Chem. 20 (2006) 74.
[14] L. Tian, B. Qian, Y. Sun, X. Zheng, M. Yang, H. Li, X. Liu, Appl. Organomet. Chem. 19 (2005) 980.
[15] L. Tian, Y. Sun, B. Qian, G. Yang, Y. Yu, Z. Shang, X. Zheng, Appl. Organomet. Chem. 19 (2005) 1127.
[16] T.S. Basu Baul, C. Masharing, S. Basu, E. Rivarola, M. Holčapek, R. Jirásko, A. Lyčka, D. de Vos, A. Linden, J. Organomet. Chem. 691 (2006) 952.
[17] L.S. Zamudio-Rivera, R. George-Tellez, G. López-Mendoza, A. Morales-Pacheco, E. Flores, H. Höpfl, V. Barba, F.J. Fernández, N. Cabirol, H.I. Beltrán, Inorg. Chem. 44 (2005) 5370.
[18] S. Gaur, N. Fahmi, R.V. Singh, Phosphorus, Sulfur Silicon Relat. Elem. 182 (2007) 853.
[19] W. Rehman, M.K. Baloch, A. Badshah, Eur. J. Med. Chem. 43 (2008) 2380.
[20] U.N. Tripathi, M.S. Ahmad, G. Venubabu, P. Ramakrishna, J. Coord. Chem. 60 (2007) 1709.
[21] M. Jain, S. Gaur, V.P. Singh, R.V. Singh, Appl. Organomet. Chem. 18 (2004) 73.
[22] M. Nath, S. Pokharia, G. Eng, X. Song, A. Kumar, M. Gielen, R. Willem, M. Biesemans, Appl. Organomet. Chem. 18 (2004) 460.
[23] M. Nath, S. Pokharia, G. Eng, X. Song, A. Kumar, Eur. J. Med. Chem. 40 (2005) 289.
[24] M. Nath, S. Pokharia, G. Eng, X. Song, A. Kumar, Spectrochim. Acta, Part A 63 (2006) 66.
[25] M. Nath, S. Pokharia, G. Eng, X. Song, A. Kumar, J. Organomet. Chem. 669 (2003) 109.
[26] M. Nath, S. Pokharia, G. Eng, X. Song, A. Kumar, Synth. React. Inorg. Met. Org. Chem. 34 (2004) 1689.
[27] M. Nath, R. Yadav, G. Eng, T.T. Nguyen, A. Kumar, J. Organomet. Chem. 577 (1999) 1.
[28] M. Nath, H. Singh, P. Kumar, A. Kumar, X. Song, G. Eng, Appl. Organomet. Chem. 23 (2009) 347.
[29] R.C. Poller, The Chemistry of Organotin Compounds, Logos Press Limited, London, 1970. p. 1–315.
[30] M. Nath, P.K. Saini, X. Song, G. Eng, J. Organomet. Chem. 693 (2008) 2271.
[31] M. Nath, X. Sulaxna, G. Song, Eng. Spectrochim., Acta Part A 64 (2006) 148.
[32] M. Nath, X. Sulaxna, G. Song, Eng. J. Organomet. Chem. 691 (2006) 1649.
[33] M. Nath, S. Goyal, Main Group Met. Chem. 19 (1995) 75.
[34] M. Nath, S. Pokharia, R. Yadav, Coord. Chem. Rev. 215 (2001) 99.
[35] M. Nath, S. Goyal, G. Eng, D. Whalen, Bull. Chem. Soc. Jpn. 69 (1996) 605.
[36] T.P. Lockhart, W.F. Manders, Inorg. Chem. 25 (1986) 892.
[37] T.P. Lockhart, W.F. Manders, J.J. Zuckerman, J. Am. Chem. Soc. 107 (1985) 4546.
[38] G.K. Sandhu, G. Kaur, J. Holeček, A. Lyčka, J. Organomet. Chem. 332 (1987) 75.
[39] B.S. Saraswat, J. Mason, Polyhedron 5 (1986) 1449.
[40] Powder Diffraction File, Sets 1–10, Joint Committee on Powder Diffraction Standards, Philadelphia, PA, 1967, p. 213, 546.
[41] G.A.A. Costa, M.C. Silva, A.C.B. Silva, G.M. de Lima, R.M. Lago, M.T.C. Sansiviero, Phys. Chem. Chem. Phys. 2 (2000) 5708.